Electronic transport properties of lead nanowires*

Lishu Zhang(张力舒), Yi Zhou(周毅), Xinyue Dai(代新月), Zhenyang Zhao(赵珍阳), and Hui Li(李辉)†

Key Laboratory for Liquid–Solid Structural Evolution and Processing of Materials, Ministry of Education, Shandong University, Jinan 250061, *China*

(Received 24 February 2017; revised manuscript received 20 April 2017; published online 6 June 2017)

Lead nanowire occupies a very important position in an electronic device. In this study, a genetic algorithm (GA) method has been used to simulate the Pb nanowire. The result shows that Pb nanowires are a multishell cylinder. Each shell consists of atomic rows wound up helically side by side. The quantum electron transport properties of these structures are calculated based on the non-equilibrium Green function (NEGF) combined with the density functional theory (DFT), which indicate that electronic transport ability increases gradually with the atomic number increase. In addition, the thickest nanowire shows excellent electron transport performance. It possesses great transmission at the Fermi level due to the strongest delocalization of the electronic state. The results provide valuable information on the relationship between the transport properties of nanowires and their diameter.

Keywords: lead nanowires, electronic transport, genetic algorithm, non-equilibrium Green function, density functional theory

PACS: 31.15.E– **DOI:** 10.1088/1674-1056/26/7/073102

1. Introduction

In the last two decades, nanowires have been a focus of material science and the condensed matter physics, because metallic nanowires display an interesting quantum phenomenon that may be exploited to generate new-generation electronic device. Lead has been applied in many parts of devices, because it is widespread, soft, dense, ductile, easy to extract, and highly malleable metal with poor conductivity.[1] Pb nanowire is superconducting and superconducting nanodevices are predominately prepared or fabricated on semiconductor substrates.[2] A great deal of progress has been made in studying the metallic nanowire and its fabricating method. For example, Yang *et al.*[3] reported a one-step methodology for the fabrication of highly conductive and stretchable Ag nanowires composite electrodes based on a high-intensity pulsed light (HIPL) technique. Repetto[4] fabricated the aluminum nanowire electrodes by defocused ion beam sputtering. Volosskiy *et al.*[5] obtained ultrathin metallic nanowires by a metal-organic framework template. These advances are very valuable to learn about the fabricating method of this kind of metallic nanowire, but they do not focus on their properties. On the nanoscale, study of the properties of nanowires is valuable because it is important for potential applications in the fields of electronics, magnetic medium, optics, thermoelectronic, sensor devices, and creating a new generation of electronic devices.[6–13] Tang *et al.*[10] adopted in-tandem *in situ* TEM and molecular dynamics (MD) simulations in order to investigate the mechanical properties and behaviors of ultrathin Si nanowires. It was revealed that the mechanical behavior of Si nanowires had been closely related to the wire diameter. Similarly, Qin *et al.*[14] performed first-principles calculations of electronic properties of silicon under strains. Silicon undergoes the semimetal–metal transition at the strain of 7%, and the Fermi velocity changes very little before this critical strain. In addition, theoretical calculation demonstrated that the Al conductance decreases by a factor of 1/4 when an inserted S atom replaces the Al atom, because the S atom can shut off the p conductance channel of Al.[15] Greil[16] had shown electrical characterization of Ge nanowires, revealing a nonconstant negative piezoresistive coefficient with resistivity change being exponentially dependent on strain, which gives experimental evidence on the band structure. Similar work is also carried out in the Ge nanowire, Zhang and his coworkers used performed Huckel theory (EHT) together with a non-equilibrium Green function (NEGF) calculation method and found that the conductance achieves a peak when voltage increases, which indicated that current flow in Ge nanowire would be easier to control.[17] In addition, by using MD, Zhang *et al.*[18] discovered that inserting C atoms into Ni nanowires can improve the resistance of nanowires, which results in a decrease in their electronic transmission channels.

Properties of nanowires whose elements belong to the IVA group have received a great deal of attention. Yet, the study of the electronic transport properties of lead nanowires has so far been inadequate. On the theoretical side, it is highly desirable to be able to simulate electron transport through nanowires from first principles to improve our understanding of this important field.[19] So far, however, the results and the contrastive analysis of these issues are limited.

Here, we use the NEGF method in combination with the

*Project supported by the National Natural Science Foundation of China (Grant No. 51671114) and the Special Funding in the Project of the Taishan Scholar Construction Engineering and National Key Research Program of China (Grant No. 2016YFB0300501).

†Corresponding author. E-mail: lihuilmy@hotmail.com

© 2017 Chinese Physical Society and IOP Publishing Ltd

density functional theory (DFT) to study the electronic transport of lead nanowires with different diameters.

2. Model and simulation methods

In this study, the devices are divided into a channel part and electrodes, as shown in Fig. 1. The nanowire is placed in the supercell at least 63 Å vacuum layer thickness between neighboring cells to stop the interaction between nanowire and its periodic image.[20,21] A genetic algorithm (GA)[20–23] method based on MD has been used to obtain the most stable geometrical structure. In the GA process, the initial configuration with arbitrary orientation is generated randomly. Any two participants in the population are chosen as parents to generate a child wire by a mating operation.[20,21] If the generated child has distinct geometry and lower energy, it would be relaxed by MD quenching and selected to replace its parents in the population. 2000–10000 GA iterations have been performed to ensure a real global minimum.

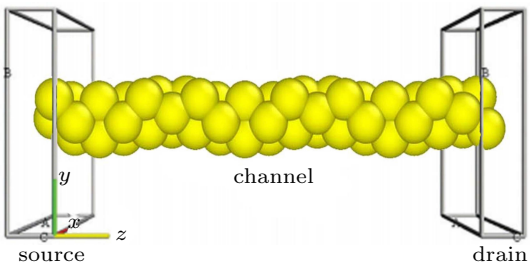


Fig. 1. (color online) The schematic of the computational models. The supercell particle number of lead nanowire is 20 and the length of electrodes is 63 Å.

The quantum electron transport properties of lead nanowires are calculated using the NEGF combined with the DFT by the softpackage Atomistix ToolKit,[18,24–26] which can simulate the electrical properties and quantum transport properties of nano structures and nano devices.[26] Double-zeta single polarized basis sets are adopted for the local atomic numerical orbitals, and norm-conserving pseudo-potentials are employed. The exchange correlation function is treated by the Perdew–Burke–Ernzerhof (LEADE)[27] generalized gradient approximition (GGA). The energy mesh cutoff is set to be 150 Ha. The k-point grid mesh is sampled by $1 \times 1 \times 100$ utilized in the Brillouin zone integration. An electron temperature is 300 K. The energy convergence criterion is set to 10^{-4} eV. The current I through the device is an integral of the electron transmission probability over the energy, which is obtained from the Landauer–Büttiker equation where the quantity $T(E,V)$ is the transmission function that describes the rate at which electrons transmit from the source to the drain contacts by propagating through the device; $f_{1,2}(E)$ denote the Fermi functions of the source and drain electrodes; e and h are the electron charge and Planck constant, respectively.

3. Results and discussion

Figure 2 shows the snapshots for some selected configurations of the lead nanowires obtained from our calculations. The radii of the nanowires are 4.6 Å, 5.3 Å, 7.7 Å, 11.1 Å, 13.2 Å, and 14.2 Å, respectively, which is denoted as wire 1, wire 2, wire 3, wire 4, wire 5, and wire 6. As for wire 1 and wire 2 in which the number of atoms is not much, their structures are non-helical. The wire 1 is chiral which features three-strand packing. The wire 2 exhibits pentagonal motifs. With the number of atoms increasing, the nanowire structures turn to the multiwalled cylinder (i.e. wire 3, wire 4, wire 5, and wire 6), which has also been found on Ti and Au nanowires.[20,21] Compared with Ti nanowires, the helical multi-walled cylindrical structure is obtained as well, but also found was pentagonal packing. This difference is clearly related to surface energy. As for lead nanowires structure, the surface of nanowires is composed by several curved layers. Each layer is formed by atom rows wound up helically side by side, and the close-packed curved layers exist in a certain extend angle, which is called curved surface epitaxy.[28,29] It is obvious that these wires have different angles.

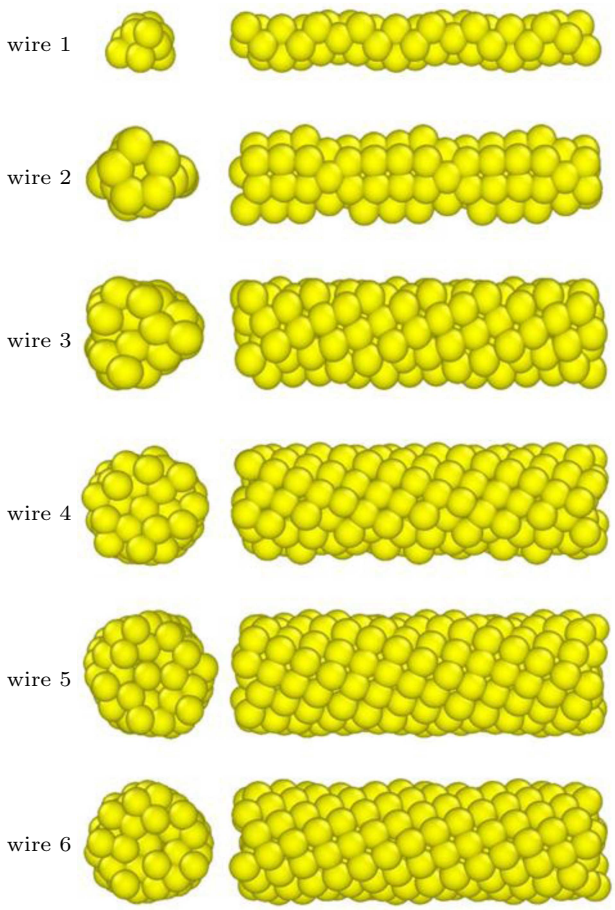


Fig. 2. (color online) Morphologies of some selected lead nanowires: wire 1, wire 2, wire 3, wire 4, wire 5, and wire 6, respectively. In each case, a top view (left) and side view (right) are presented.

It is expected that such a unique structure would have novel electronic properties. To shed light on the electronic

transport properties of these wires, we examined the current–voltage (I–V) characteristic curves to represent the electronic transport probability of lead nanowires. Figure 3 shows the I–V characteristic curves of the six lead nanowires. The spin-polarized current through nanowire is only several microamperes,[28] while in this study, the current through nanowires is several thousand microamperes. The transport current is far more than the spin-polarized current. Although spin-polarized transport occurs naturally in any metallic nanowires including lead nanowires,[29] the polarization does not influence the current in this work. Interestingly, all these curves are nonlinear, not showing a typical Ohmic patteren. Zhang *et al.*[17] have EHT together with NEGF to study the I–V characteristics of germanium nanowires, who found that under a high applied bias, the I–V curve is nonlinear. The slope of the I–V curve is the conductance in which the fluctuation can be influenced by the resonant tunneling of nanowires. It is suggested that the resonant tunneling is responsible for the standing waves. These standing waves with large amplitudes of the wave function of the nanowires lead to the nonlinear characteristic of the I–V curves.[30] The nonlinear I–V curve is caused by the quantum size effect of the nanowire. It can be seen that the maximum current of wire 6 is much larger than that of wire 1. As the particle number increases, the current value increases, which indicates that the number of atoms can strongly influence the I–V curves. The inset of Fig. 3 displays the differential conductance ($\mathrm{d}I/\mathrm{d}V$ curves) of the six nanowires which are also nonlinear. The wire 6 has the maximum conductance at 0.25 V, which does not follow Ohm's law, but follows the law that the greater the cross-sectional area is, the greater the conductivity is. Interestingly, we can observe that wire 2 has the lowest current in six devices. The performance of the transmission spectrum gives a reasonable explanation of the phenomenon that the current of wire 2 is the lowest in six devices. We can learn

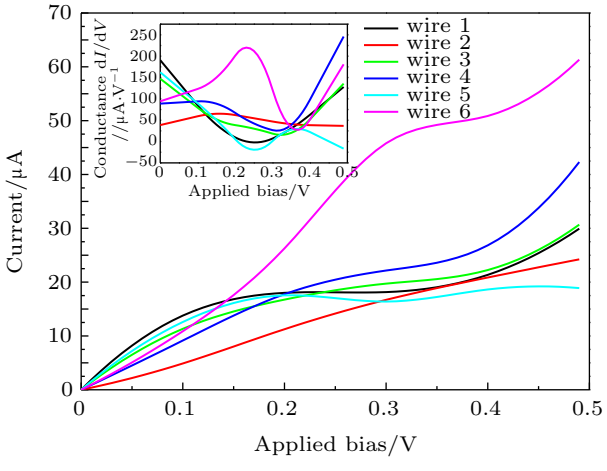


Fig. 3. (color online) I–V characteristic curves of lead nanowires with different diameter. The inset is the conductance spectra of the six lead nanowires.

from the electronic transmission spectrum of the nanowires that at free applied bias (see Fig. 4), the wire 2 has the wave trough around Fermi level, indicating that the value of the I–V curve would be weak. Compared to other wires which have the wave trough around the Fermi level as well, the value of the wire 2 valley is inferior to other wires, which is consistent with I–V curves.

The transmission profiles of these nanowires are shown in Fig. 4. The transmission at each energy point is calculated by summing up the transmission eigenvalues of every electron transport channel,[31] which are obtained by diagonalizing the transmission matrix. Different from molecular devices that exhibit step-like and discrete transmission spectra, the transmission spectra of these lead nanowires are continuous, showing a value beyond 1 in some energy ranges as well due to the continuous and degenerate energy levels of lead nanowires. At the zero bias, the large transmission coefficient at E_{F} means the strong transport capacity. It is found that the significantly stronger transmission at E_{F} is observed for the wire 1 as well as wire 2, just as shown obviously in Fig. 4. As for these wires with different diameters, the comparison of the transmission values can be expressed as $1 > 2 > 3 > 4 > 5 > 6$. To estimate the transmission at E_{F}, the dominant eigenstate of the transmission matrix at E_{F} is calculated and displayed in the insets of Figs. 4(a)–4(f). Notably, the transmission eigenstates of wire 4, wire 5, and wire 6 show delocalized throughout the whole central region, resulting in the pronounced transmission at E_{F}. Whereas, the wire 1 shows localization and the molecule has a weak electronic state, as well as the wire 2 and wire 3, causing weaker transmission than the wire 4, wire 5, and wire 6. In general, the wire has a stronger electronic state, leading to a larger transmission value of the wire than others. Although the distribution of the electronic state of the wire 1 is similar to the devices 2 and 3, obviously there is no spread of the electronic state on the center between the left and right electrodes, which brings about the weakest transmission of the wire 1 for these nanowires.

We further decomposed the electronic transmission at the Fermi level of these wires as shown in Table 1. The number of eigenvalue characterizes the number of channels. For wire 1, it has two spin up electronic transmission channels, showing a transmission probability of about 1.0. Meanwhile, wire 2 is observed to have three electronic transmission channels and transmission probability around 1.0, which results in the pronounced transmission at E_{F}. Wire 3 has the largest number of channels, while wire 4 has only one electronic transmission channel and the eigenvalue is about 1, which makes wire 4 not have significant transmission at E_{F}. In general, it can be seen that the transmission value increases with the increase of the atomic number. In addition, near the Fermi level, a significant peak appears which exhibits semiconducting and pure metallic properties.

Table 1. The transmission eigenvalues of lead nanowires with different diameter.

Wire	Transmission eigenvalues					
wire 1	0.9999992	0.9999963				
wire 2	0.9999980	0.9999860	0.9998507			
wire 3	0.9999986	0.9999980	0.9999951	0.9999737	0.9999448	0.09993265
wire 4	0.9999930					
wire 5	0.9999982	0.9998553	0.9999821	0.9999277		
wire 6	0.9999999	0.9999994	0.9999898	0.9999602	0.9999868	

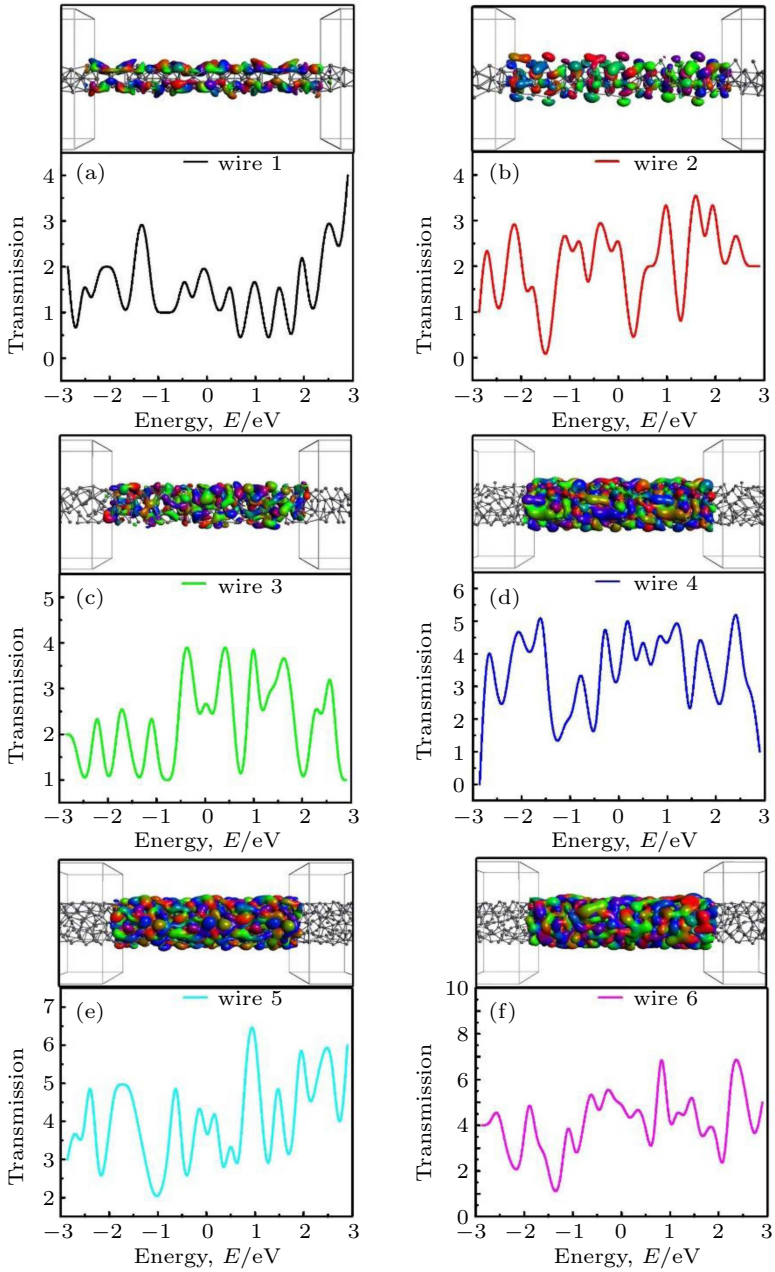


Fig. 4. (color online) The electronic transmission spectrum of the nanowires at free applied bias (0.0 V). Each inset shows their isosurface plots of the transmission eigenstates at E_F.

To further explore more electronic transmission properties, figure 5 shows that the densities of states (DOSs) of these lead nanowires near the Fermi energy level are different. The modes are different as well, leading to the discrepancy of the transmission spectrum.

As for wire 1, there is one prominent peak at −2.16 eV in the valence band region and some weak peaks in the conduction band region, out of which the highest magnitude peak appears at about 1.48 eV. The DOS of wire 2 shows few strong peaks in the valence band region, out of which the highest one

appears at −1.6 eV and a strong peak also appears in the conduction band region at 0.76 eV, which defends less localization of states near the Fermi level. While for wire 3, a significant peak appears in the conduction band and a weak peak at 0.1 eV very close to the Fermi level. As for wire 4, there is one prominent peak at −0.7 eV in the valence band region and some weak peaks in the conduction band region, out of which the highest magnitude peak appears at 2.4 eV. For wire 5, the highest peak appears at −2.34 eV near the Fermi level and a prominent peak exists at 1.5 eV in the conduction band region which defends less localization of states near the Fermi level. The DOS for wire 6 shows few strong peaks in the valence band region, out of which the highest one appears at −0.24 eV and a strong peak also appears in the conduction band region at 2.08 eV, which defends less localization of states near the Fermi level.

We further computed projected DOS (PDOS) as shown in Fig. 6, from which we can conclud that DOS is mainly consisted by p orbitals, which is supported by the result in Si, Ge, and Sn nanowires.[17] It is worth noting that the peaks of PDOS are different with different diameters. It can be explained by the rule that all physical properties are obtained by calculating the expected value of the wave function. That is $\langle 1|P|2\rangle$, where P is one of the quantities. When one presents the Px orbital channel of atoms, that means PDOS. So, from this point, the Px orbital channel is actually a spherical harmonic function. When the diameter of the device gets changed, the spherical harmonic function would change as well, which leads to the different PDOS peaks.

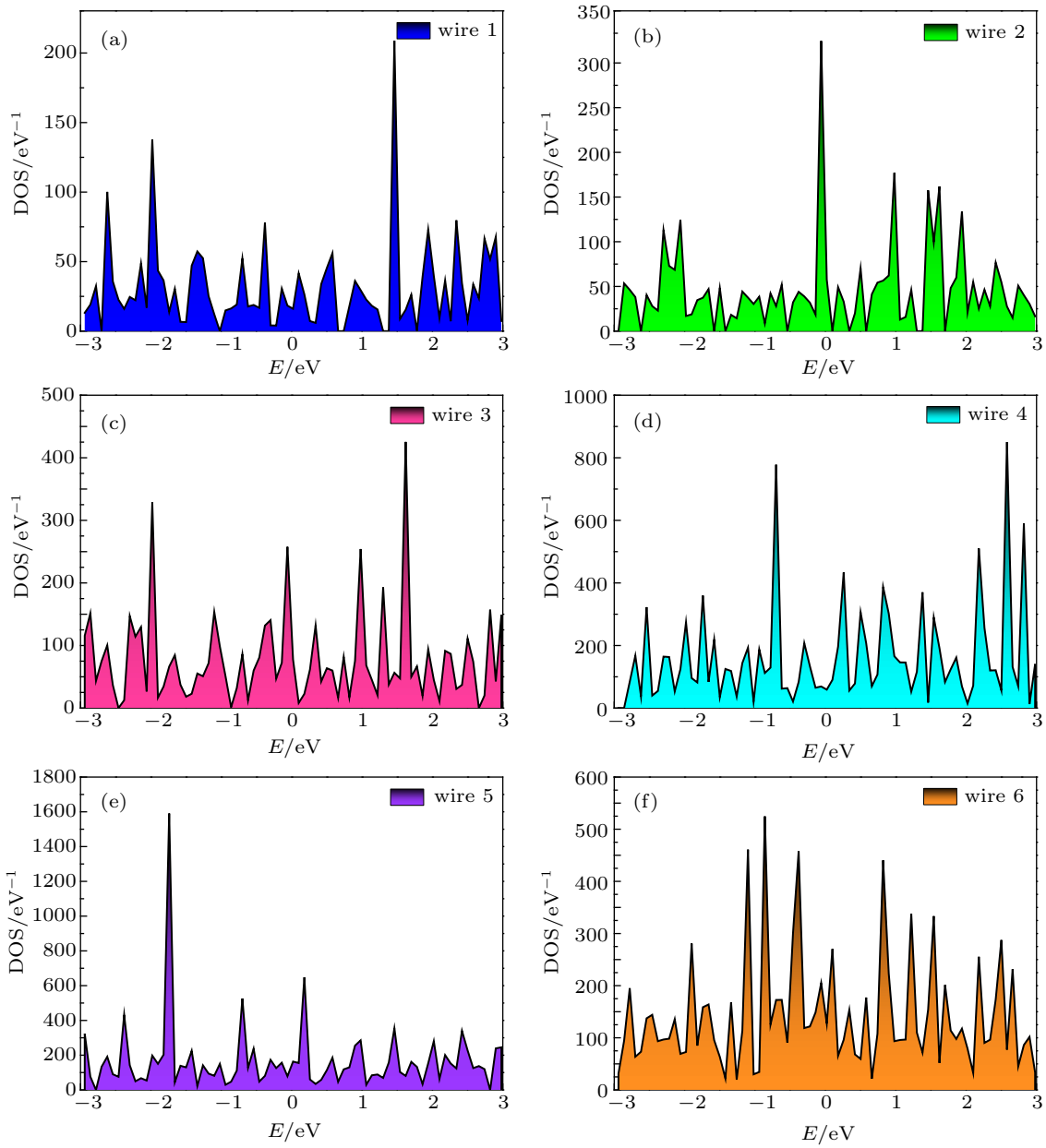


Fig. 5. (color online) DOSs for (a) wire 1, (b) wire 2, (c) wire 3, (d) wire 4, and (e) wire 5. The zero of energy axis is the Fermi level.

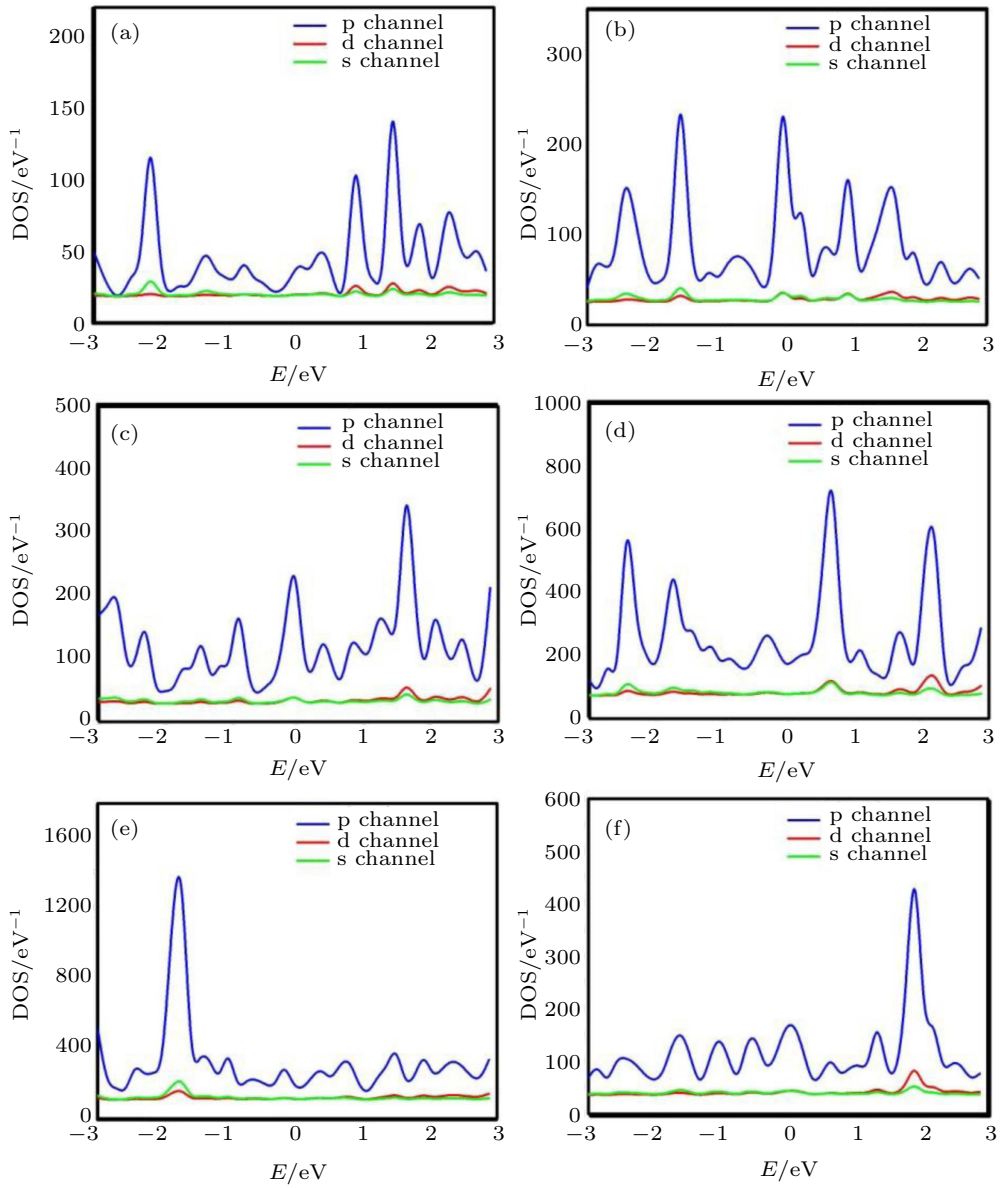


Fig. 6. (color online) PDOSs for (a) wire 1, (b) wire 2, (c) wire 3, (d) wire 4, and (e) wire 5. The zero of energy axis is the Fermi level.

Si, Ge, Sn, and Pb are in the same main group in the periodic table of elements. Therefore, their structures and properties may be similar in some extent. We can learn from the previous work that these four kinds of nanowires are all spiral winding and get shifted as the diameter changes. Compared to the result from the research of Zhang,[17] the conductance spectrum (G–V) of the Pb nanowire is quite different from those of Sn, Si, and Ge nanowires. In the same range from 0 to 0.5 V, the Pb device has a more stable conductivity than that of other element devices and does not show a negative differential resistance (NDR) effect. That is because that the conductance spectra of Si, Ge, and Sn nanowires have many irregular peaks, and the transmission spectra of Pb nanowires do not show the gap around Fermi level while the other three do. We conclude that Pb nanowire has more stable electrical properties, indicating that Pb nanowire would be a better candidate for the new generation of nanowire transistors.

4. Conclusion

We investigate the structures and electronic transport properties of lead nanowires by the GA process and the NEGF method with the DFT frame. Helical structures with different helix degrees are found in lead nanowires. Due to the quantum size effect, the I–V characteristic curves of the nanowires are nonlinear, which do not follow Ohm's law. The thickest nanowire shows great transmission at the Fermi level because of the strong delocalized electronic state. In addition, the transmission spectrum and DOS show that transmission properties are dependent on the diameter of the nanowires. The nanowire with the maximum diameter has excellent performances, holding promising application in electronic devices. This study provides insight into the relation between the trans-

port property and the diameter of nanowires.

References

[1] Srivastava A, Tyagi N and Singh R 2011 *Mater. Chem. Phys.* **127** 489
[2] Wang J, Jia J F, Ma X C, Shen Q T, Han T Z, Jin A Z, Lu L, Gu C Z, Tian M L and Xie X 2010 *J. Vac. Sci. Technol. B* **28** 678
[3] Yang Y, Ding S, Araki T, Jiu J, Sugahara T, Wang J, Vanfleteren J, Sekitani T and Suganuma K 2016 *Nano Res.* **9** 401
[4] Repetto D, Giordano M C, Martella C and Mongeot F B 2015 *Appl. Surf. Sci.* **327** 444
[5] Volosskiy B, Niwa K, Chen Y, Zhao Z, Weiss N O, Zhong X, Ding M and Lee C 2015 *ACS Nano* **9** 3044
[6] Wang K, Meng Q, Zhang Y, Wei Z and Miao M 2013 *Adv. Mater.* **25** 1494
[7] Wang Q, Wang X, Liu B, Yu G, Hou X, Chen D and Shen G 2013 *J. Mater. Chem. A* **1** 2468
[8] Terrones M 2013 *Int. Mater. Rev.* **49** 325
[9] Zheng G, Cui Y, Karabulut E, Wåberg L, Zhu H and Hu L 2013 *MRS Bull.* **38** 320
[10] Tang D M, Ren C L, Wang M S, Wei X, Kawamoto N, Liu C, Bando Y, Mitome M, Fukata N and Golberg D 2012 *Nano Lett.* **12** 1898
[11] Li M, Zhang H Y, Guo C X, Xu J B and Fu X J 2009 *Chin. Phys. B* **18** 1594
[12] Kocakaplan Y and Kantar E 2014 *Chin. Phys. B* **23** 046801
[13] Li S, Huang G Y and Guo J K 2017 *Chin. Phys. B* **26** 027305
[14] Qin R, Wang C H, Zhu W and Zhang Y 2012 *AIP Adv.* **2** 022159
[15] Lang N D 1995 *Phys. Rev. B* **52** 5335
[16] Greil J, Lugstein A, Zeiner C, Strasser G and Bertagnolli E 2012 *Nano Lett.* **12** 6230
[17] Zhang X, Li H and Liew K M 2007 *J. Appl. Phys.* **102** 073709
[18] Zhang L, Wu W, Zhou Y, Ren H, Dong J and Li H 2016 *Phys. Chem. Chem. Phys.* **18** 5336
[19] Li H, Zhang X, Sun F, Li Y, Liew K M and He X 2007 *J. Appl. Phys.* **102** 013702
[20] Wang B, Yin S, Wang G, Buldum A and Zhao J 2001 *Phys. Rev. Lett.* **86** 2046
[21] Wang B, Yin S, Wang G and Zhao J 2001 *J. Phys. -Condens. Matter* **13** L403
[22] Deaven D M and Ho K M 1995 *Phys. Rev. Lett.* **75** 288
[23] Mao C, Solis D J, Reiss B D, Kottmann S T, Sweeney R Y, Hayhurst A, Georgiou G, Iverson B and Belcher A M 2004 *Science* **303** 213
[24] Srivastava A, Jain S and Nagawat A 2013 *Quantum Matter* **2** 469
[25] Dong J and Li H 2012 *J. Phys. Chem. C* **116** 17259
[26] Zeng J, Chen K Q, He J, Zhang X J and Sun C Q 2011 *J. Phys. Chem. C* **115** 25072
[27] Perdew J P, Burke K and Ernzerhof M 1996 *Phys. Rev. Lett.* **77** 3865
[28] Gülseren O, Ercolessi F and Tosatti E 1998 *Phys. Rev. Lett.* **80** 3775
[29] Bilalbegović G 1998 *Phys. Rev. B* **58** 15412
[30] Shi X, Dai Z, Zhong G, Zheng X and Zeng Z 2007 *J. Phys. Chem. C* **111** 10130
[31] Li H, Liew K M, Zhang X, Zhang J, Liu X and Bian X 2008 *J. Phys. Chem. B* **112** 15588